Internal Conversion in the Membrane-Supported SOFC

ECS Transactions, 103 (1) 211-219 (2021)
10.1149/10301.0211ecst ©The Electrochemical Society

Internal Conversion in the Membrane-supported SOFC

A. V. Samoilov[a,b], D. A. Agarkov[b,a], Yu. S. Fedotov[a,b], S. I. Bredikhin[a,b]

[a] Laboratory of Spectroscopy of Defect Structures, Osipyan Institute of Solid State Physics RAS, Chernogolovka, Moscow region 142432, Russia
[b] Laboratory of Fuel Cells, Moscow Institute of Physics and Technology, Dolgoprudny, Moscow region 141701, Russia

Abstract

Studies of the internal methane conversion process were carried out on an experimental short stack of two 100x100 mm electrolyte-supported SOFCs. A whole series of experiments were carried out on H_2+CH_4+H_2O mixtures with different sets of conditions – an increase in the ratio and consumption of methane, and then a decrease in temperature.

The results of experiments at an operating temperature of 850°C showed that the kinetics of internal conversion was largely underestimated. The assembly of two SOFCs converts methane up to concentrations not exceeding the calculated equilibrium ones, up to the maximum available flow rate on the equipment used – 187 ml/min – even without current passing. This fuel flow rate can provide a current of up to 53 A, while the rated operating current of these SOFCs is about 20 A, up to 30 A on methane-rich fuel. The current further stimulates the conversion by generating additional steam.

Introduction

Steam reforming is a well-known process for producing hydrogen or hydrogen-containing gas (synthesis gas) from methane or other hydrocarbon fuels. For methane, the conversion process [1], accompanied by the shift reaction [2], proceeds on the surface of the catalyst, which is most often nickel:

$$CH_4 + H_2O \leftrightarrow CO + 3H_2 \qquad (\Delta H_{298} = 206.1\ kJ/mol) \qquad [1]$$

$$CO + H_2O \leftrightarrow CO_2 + H_2 \qquad (\Delta H_{298} = -41.15\ kJ/mol) \qquad [2]$$

Steam reforming of methane is a highly endothermic reaction. According to thermodynamic calculations, the equilibrium in equation [1] shifts towards the reaction products at high temperatures and low pressures. Similarly, to equation [1], similar reactions can be written for other hydrocarbons. In addition to these reactions, undesirable reactions also occur which is reducing the yield of hydrogen and leading to the precipitation of carbon:

$$CO + H_2 \leftrightarrow C + H_2O \qquad (\Delta H_{298} = -131.29\ kJ/mol) \qquad [3]$$

$$2CO \leftrightarrow C + CO_2 \qquad (\Delta H_{298} = -172.42\ kJ/mol) \qquad [4]$$

$$CH_4 \rightarrow C + 2H_2 \qquad (\Delta H_{298} = 74.87\ kJ/mol) \qquad [5]$$

The practical minimum steam/carbon ratio required to prevent unwanted reactions [3-5] is usually above 1.7 for natural gas. Typically, steam reforming catalysts are Group VIII metals, in which nickel is most commonly used. Catalysts based on rhodium, ruthenium and other noble metals are more active, but due to their cost, they are not used. Nickel catalysts have proven their effectiveness due to the simplicity of their manufacture, stability, and chemical activity (1). On such catalysts, the products of steam reforming are determined by the thermodynamic equilibrium established between equations [1-5].

It has long been known that the heat required for the endothermic methane conversion process can be provided by an electrochemical reaction in a stack (2,3). This has led to the development of various concepts for internal reforming in high temperature solid oxide fuel cells. There are two main approaches, which are called direct and indirect internal reforming. Indirect reforming is the conversion of methane using reformers in close thermal contact with the stack. So, for example, in (4), plate reformers alternate with planar membrane-electrode assemblies (MEA). Conversion products from each reformer are fed to adjacent cells. Thus, the advantages of indirect internal reforming are close thermal contact between the stack and the reformer as well as the absence of soot formation at the anode of the fuel cell, and the disadvantages are that heat is well transferred only from the MEA adjacent to the reformer, and steam for the conversion process must be supplied separately. A variation of this approach is the placement of the reforming catalyst in the gas distribution units of the stack (1). Thus, in the process of indirect internal reforming, the methane steam reforming reaction and the electrochemical reactions in the MEA are separated.

With direct internal reforming, the process of steam reforming of methane proceeds directly at the anode of a solid oxide fuel cell due to the high operating temperature and the presence of nickel in the composition (5,6). The advantage of direct reforming is not only thermal, but also chemical integration – the water vapor produced during the anodic electrochemical reaction can be used for reforming without the need for anode recycling. Also, the endothermic effect of steam reforming can be used to control the temperature of the stack, but they cannot completely compensate for the heat generated by the electrochemical reaction. In addition, difficulties arise in controlling the temperature gradient along the length of the anode chamber (7). An example of using direct internal reforming is a prototype of a 25 kW SOFC power plant (8) presented by Westinghouse. On the other hand, the same work indicates that due to temperature gradients, it is impossible to convert more than 30% of methane.

In work (9) it is shown that, supplying 30% methane to the electrolyte-supported stack at the input, 22% is observed at the output. Thus, based on the literature data, a high conversion rate in the process of internal methane reforming cannot be expected.

Solid oxide fuel cells (SOFCs) and power plants based on them are among the most efficient (10), eco-friendly (11) as well as reliable (12) power sources. SOFC electrical efficiency lies in a range of 55-60%, combined heat and power efficiency exceeds the

value of 85%. Hybrid systems with gas and steam turbines give opportunity to further increase of mentioned efficiency levels (13-14).

Research team at Osipyan Institute of Solid State Physics RAS works on research and development tasks in a field of solid oxide fuel cells and power plants based on them. This works lie in different directions from search for new electrolyte (15) and electrode (16) materials via investigation of electrode processes (17-18), as well as manufacture of membrane-electrode assemblies (19-20), search for sealing glasses (21), construction of SOFC stacks and fuel processors (22) up to power plant design, manufacture and testing.

In previous works synthesis gas containing of hydrogen and nitrogen was used as fuel for SOFC stacks based on electrolyte and anode supported MEAs. Synthesis gas was prepared in external devices: mixed artificially using compositions measured from fuel processors or prepared in external fuel reformers. In this work studies of the internal methane conversion process were carried out on an experimental short stack of two 100x100 mm electrolyte-supported SOFCs. It was shown that assembly of two SOFCs converts methane up to concentrations not exceeding the calculated equilibrium ones, up to the maximum available flow rate on the equipment used – 187 ml/min – even without current passing.

Experimental Setup

A schematic of the experimental setup for researching the internal conversion process on electrolyte-supported SOFC membrane-electrode assemblies is shown in figure 1.

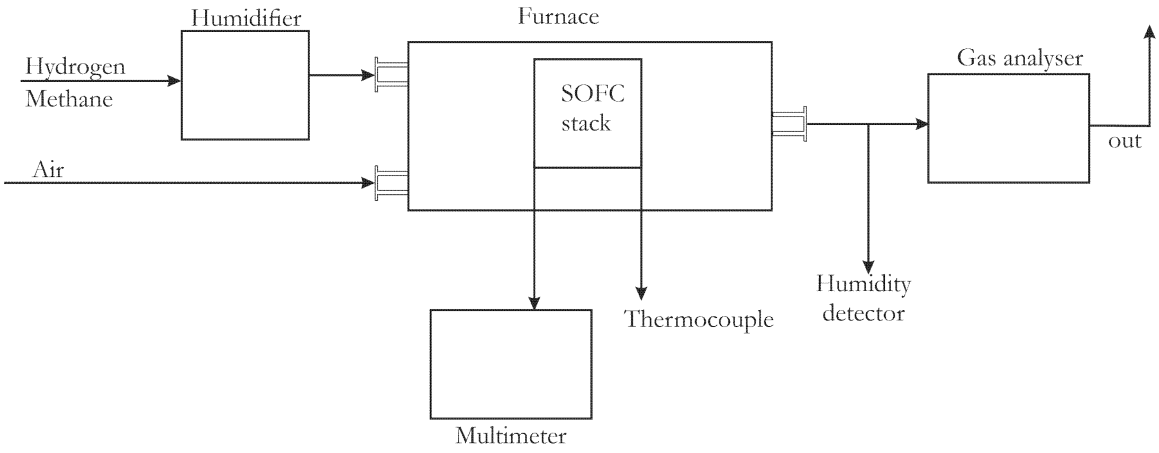

Figure 1. Schematic of the experimental setup for researching the internal conversion process on electrolyte-supported SOFC membrane-electrode assemblies.

The principle of operation of the experimental setup is as follows: with the help of mass-flow controllers (MFC), the required consumption of fuel and oxidizer is set. The fuel is passed through a humidifier to achieve the required moisture content. Then the fuel and oxidizer are fed to the assembly of electrolyte-supported SOFCs located in the furnace.

The assembly temperature is monitored with a thermocouple and the open circuit voltage is monitored with a Fluke multimeter. The exhaust gases are supplied to the gas analysis stand, having previously passed through a humidity sensor. The stand includes Siemens gas analyzers with the help of which the composition of exhaust gases is monitored.

Results and Discussion

Internal conversion tests were carried out at the operating temperature of the electrolyte-supported SOFCs – 845ºC.

A hydrogen-containing gas with the composition of 94.9% H_2; 0.21% O_2; 0.06% CO was taken as a reference point (figure 2a) (flow rate 450 ml/min). The measured humidity at the entrance to the assembly was 6.4%, at the outlet from the assembly it was 7.6%. The open circuit voltage was 1.054 V. To study the heat effect of the reaction, the temperature of the assembly inside the furnace was measured. When pure hydrogen is supplied, the temperature is 845 °C.

To study the internal conversion process, methane was gradually added to hydrogen. First, 2.4% (on a dry mixture) of methane (11.26 ml/min) was added to the available hydrogen (flow rate 450 ml/min). The composition of the gas at the outlet is 91.78% H2; 0.18% O_2; 2.27% CO; 0.13% CO_2; 0.06% CH_4 (figure 2b). The humidity measured at the outlet from the assembly dropped from 7.6% to 5.5%. The assembly temperature dropped from 845°C to 844°C. The open circuit voltage increased from 1.054 V to 1.08 V. Observed processes indicate the beginning of the internal methane conversion process.

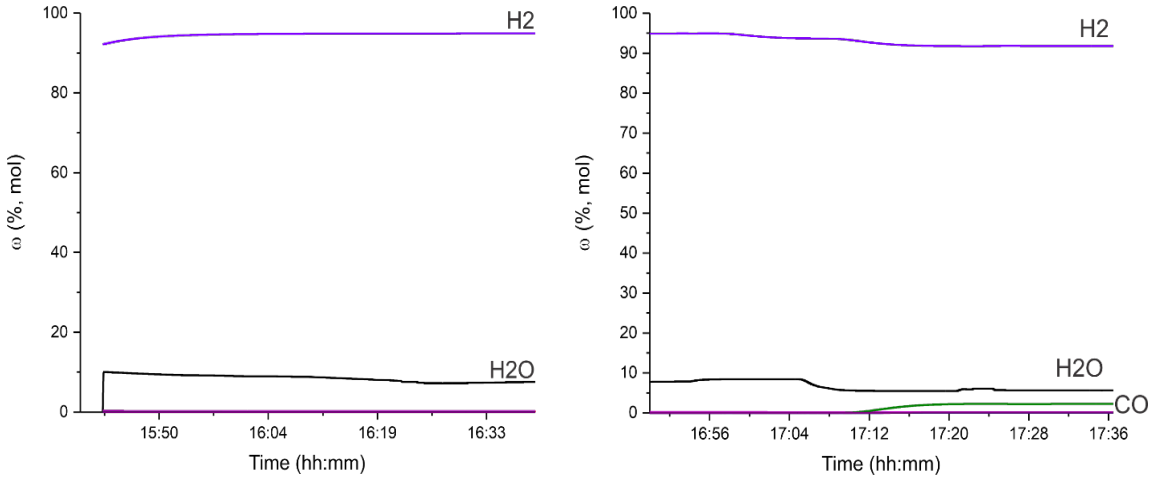

Figure 2. Composition of gas at the outlet of the gas analyzer. Fuel: a – pure hydrogen; b – hydrogen + 2.4% of methane.

Then, the proportion of methane (26.86 ml/min) in a mixture with hydrogen (450 ml/min) was increased to 5.6% (on a dry mixture). The composition of the gas at the outlet is shown in figure 3a – 89.69% H_2; 0.16% O_2; 4.74% CO; 0.12% CO_2; 0.29% CH_4. The humidity measured at the outlet from the assembly continued to decrease to 2.7%.

The temperature remained unchanged (844°C). The open circuit voltage for the upper MEA increased even further – to 1.14 V. Due to the fear of the start of the soot formation process with a further increase in the methane content in the mixture and to check the influence of the anode current on the conversion process, the assembly was stabilized under a current of 10 A. At the same time, the composition of the gas at the outlet changed as follows – 86.82% H_2; 0.15% O_2; 4.91% CO; 2.14% CO_2; 0.02% CH_4 (figure 3b). An increase in the concentration of carbon dioxide is observed, which may be associated with the occurrence of the shift reaction and a decrease in the concentration of methane.

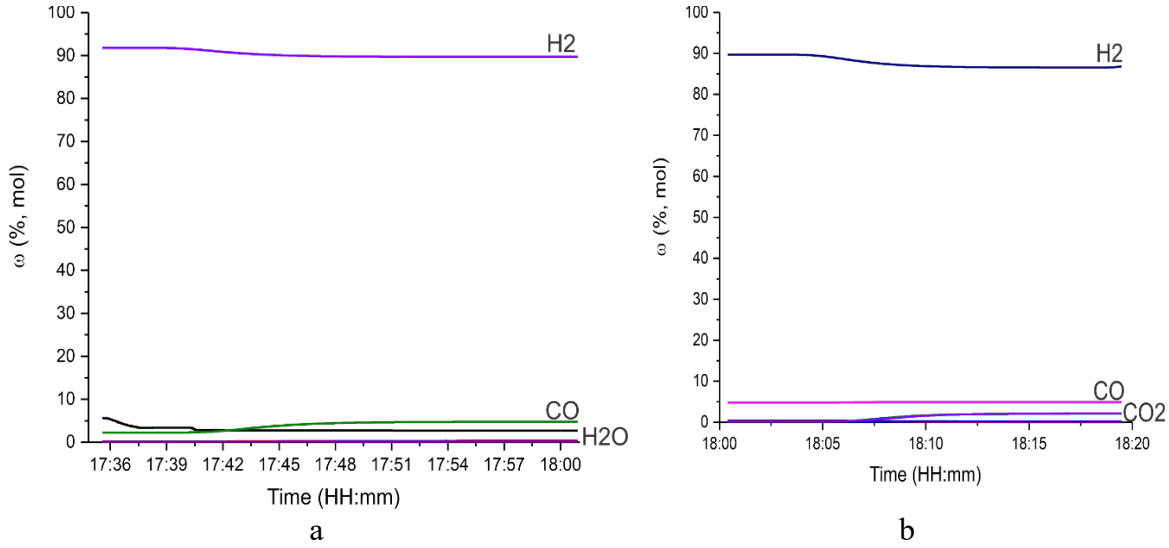

Figure 3. Composition of gas at the outlet of the gas analyzer. Fuel – hydrogen + 5.6% methane. a – without current; b – under current of 10 A.

For further experiments, the humidity was increased from 6.7% to 19.4%. The amount of methane (62.33 ml/min) in the supplied mixture with hydrogen (450 ml/min) was also increased to 12.1% (on a dry mixture). The gas composition at the outlet of the assembly is as follows: 84.55% H_2; 0.13% O_2; 10.67% CO; 1.07% CO_2; 0.13% CH_4 (figure 4a). The measured humidity at the outlet from the assembly drops from 36% (the value at the previous point is under 10 A) to 11.7%. The assembly temperature decreased to 843°C, and the open circuit voltage (upper MEA) increased from 0.993 V (without methane) to 1.027 V. As before, the assembly converts all methane supplied to it as the residual measured concentration does not exceed the values calculated from the thermodynamic balance.

At the next point, we continued to increase the concentration of methane (86.28 ml/min) in the inlet mixture with hydrogen (450 ml/min) and brought it to 16.1% (on a dry mixture). Outlet gas composition was following: 81.46% H_2; 0.16% O_2; 12.46% CO; 0.62% CO_2; 0.5% CH_4. The measured humidity at the outlet from the assembly decreased from 11.7% to 3.7%. The temperature also dropped to 842°C, and the open circuit voltage rose from 1.027 V to 1.066 V.

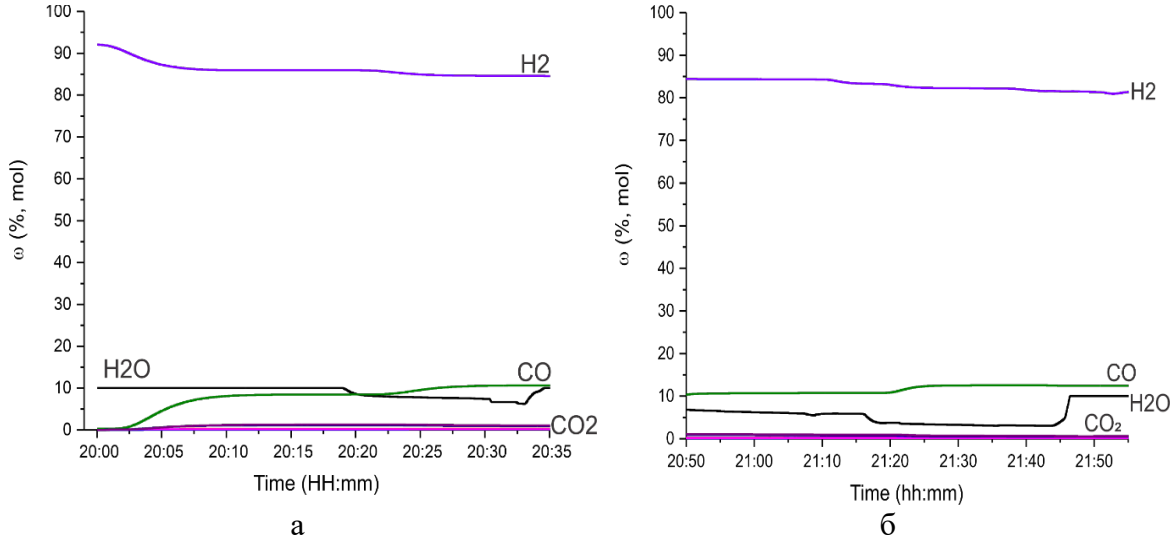

Figure 4. Composition of gas at the outlet of the gas analyzer. Fuel: a – hydrogen + 12.1% of methane; b – hydrogen + 16.1% of methane.

At the next point, it was decided to reduce the methane content (86.28 ml/min) in a mixture with hydrogen (450 ml/min) to 15.3% (on a dry mixture). The composition of the gas at the outlet is 85.56% H_2; 0.15% O_2; 10.75% CO; 0.55% CO_2; 0.22% CH_4 (figure 5a). According to thermodynamic calculations, the equilibrium fraction of methane on dry gas for the measured input composition (15.3% methane + 84.7% hydrogen) is 0.25%. That is, the measured result is even slightly below equilibrium. The measured humidity at the outlet from the assembly has slightly decreased from 3.7% to 3.67%. The assembly temperature continued to decrease and reached 840°C, and the open circuit voltage increased from 1.066 V to 1.078 V.

After that, due to the impossibility of further increasing the proportion of methane in the mixture (low output humidity as an indirect sign of the threat of soot formation and a decrease in assembly characteristics), it was decided to increase the consumption of methane (187 ml/min) and hydrogen (1059.6 ml/min) while maintaining the same proportions for dry mix (85% H_2 + 15% CH_4). However, the composition of the outlet gas changed slightly: 87.16% H_2; 0.15% O_2; 10.54% CO; 0.45% CO_2; 0.24% CH_4 (figure 5b). The measured humidity at the outlet of the assembly slightly decreased from 3.67% to 3.15% The temperature of the assembly continued to drop and reached 838°C, and the voltage of the upper MEA slightly decreased from 1.078 V to 1.076 V. Results of tests and thermodynamic calculations for a composition of 85% hydrogen + 15% methane are given in Table I.

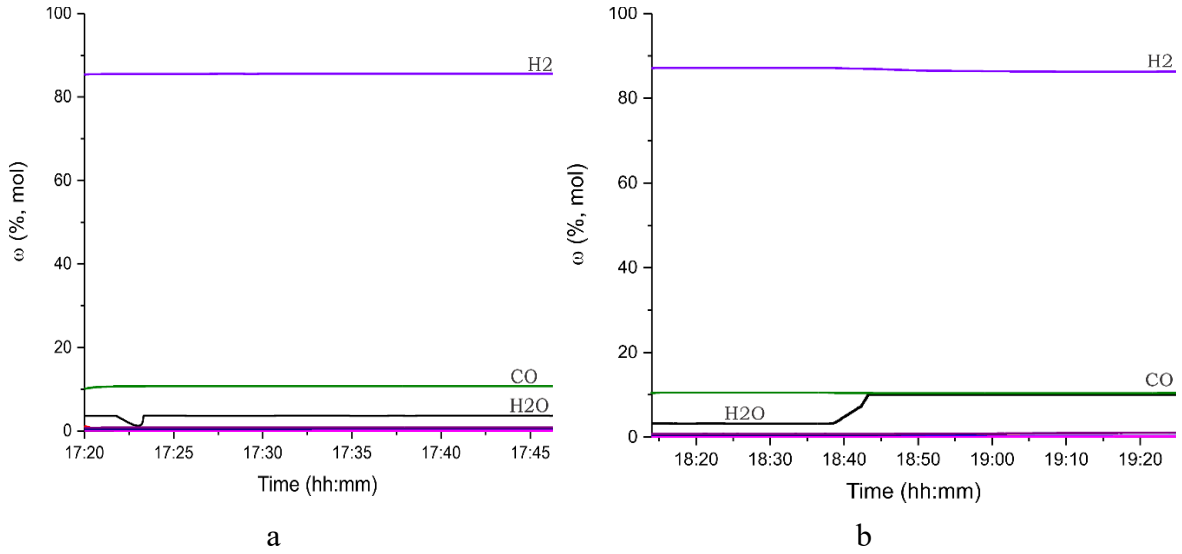

Figure 5. Composition of gas at the outlet of the gas analyzer. Fuel: a – 450 ml/min H_2 + 86.28 ml/min CH_4; b – 1059.6 ml/min H_2 + 187 ml/min CH_4.

TABLE I. Results of tests and thermodynamic calculations. Composition: 85% hydrogen + 15% methane.

	H_2O, %	H_2, %	CO, %	CO_2, %	CH_4	%C	%H	%O
Inlet	19.4	68.51	0	0	12.09	4.73	87.68	7.59
Outlet	3.05	86.06	10.22	0.436	0.233	5.33	87.74	6.93
Estimation	5.62	84.6	8.98	0.55	0.257			

It can be seen from the table that the proportion of carbon in the balance increases due to a decrease in the proportion of oxygen. The methane yield is not higher than equilibrium at the measured temperature. Thus, the results of experiments at an operating temperature of 850°C showed that the kinetics of internal conversion was largely underestimated. The assembly of two MEA converts methane to concentrations not exceeding the calculated equilibrium ones, up to the maximum available flow rate on the equipment used – 187 ml/min – even without passing current. This flow rate is capable of providing a current of up to 53 A, while the rated operating current of these MEA is about 20 A, up to 30 A on rich fuel. That is, the conversion capabilities of our MEA from these data, even in the absence of current, are at least twice their own needs. The current further stimulates the conversion by generating additional steam.

Conclusions

Thus, in the course of the experiments, it was not possible to obtain methane concentrations in the exhaust gas that significantly exceed the equilibrium ones. This result turned out to be extremely unexpected and undoubtedly positive, since it demonstrates an extremely high potential of internal conversion and opens the way to a sharp decrease in the requirements for the degree of conversion of fuel supplied to SOFC, abandonment of a bulky fuel processor, reduction of costs for SOFC cooling and, thereby,

an increase in efficiency, and reduction of mass and dimensions of power plants based on SOFCs.

Acknowledgments

This work was supported by Russian Scientific Foundation grant 17-79-30071 "Scientifically grounded optimization of power and mass-dimensional characteristics of planar SOFC stacks and development of fuel processor for highly-efficient transport and stationary power plants".

References

1. Tokyo Gas Co. Ltd., *Japanese Patent No.* **JP 06-243881** (1994).
2. A.H. Fakeeha, F.A. Abd El Aleem, and H.M. Ettouney, *J. King Saud Univ.*, **7**, Eng. Sci. (Special Issue), 171 (1995).
3. S.H. Clarke, A.L. Dicks, K. Pointon, T.A. Smith, and A. Swann, *Catal. Today*, **38,** 411 (1997).
4. K. Sato, T. Tanaka, and T. Murahashi, *1990 Fuel Cell Seminar Abstr.*, **40**, 40 (1990).
5. A.L. Dicks, *J. Power Sources*, **71**, 111 (1998).
6. В.А. Собянин, *Ж. Рос. хим. об-ва им. Д.И. Менделеева,* **XLVII,** 6, 62 (2003).
7. C.M. Finnerty, N.J. Coe, R.H. Cunningham, and R.M. Ormerod, Catal. Today, **46**, 137 (1998).
8. S. Takeuchi, A. Kusunok, H. Matsubara, Y. Kikuoka and J. Ohtsuki, *Proc. 3rd Int. Symp. Solid Oxide Fuel Cells*, **HI**, 4, 678 (1993).
9. J. Kupecki, K. Motylinski, J. Milewski, *Energy Proc.*, **105**, 1700 (2017).
10. G. Vialetto, M. Noro, P. Colbertaldo, and M. Rokni, *Int. J. Hydrog. Energ.*, **44**(19), 9609 (2019).
11. S. Kim and K.C. Kim, *Proc.*, **2**(11), 605 (2015).
12. M. Hauth, V. Lawlor, P. Cartellieri, C. Zechmeister, S. Wolff, C. Bucher, J. Malzbender, J. Wei, A. Weber, and G. Tsotridis, *ECS Trans.*, **78**(1), 2231 (2017).
13. A.V. Akkaya, B. Sahin, and H.H. Erdem, *J. Hydrog. Energy*, **33**(10), 2566 (2008).
14. T.W. Song, J.L. Sohn, T.S. Kim, and S.T. Ro, *J. Power Sources*, **158**(1), 361 (2006).
15. D.A. Agarkov, M.A. Borik, S.I. Bredikhin, A.V. Kulebyakin, I.E. Kuritsyna, E.E. Lomonova, F.O. Milovich, V.A. Myzina, V.V. Osiko, E.A. Agarkova, and N.Yu. Tabachkova, *Russ. J. Electrochem.*, **54**(6), 459 (2018).
16. V.A. Kolotygin, E.V. Tsipis, A.I. Ivanov, Y.A. Fedotov, I.N. Burmistrov, D.A. Agarkov, V.V. Sinitsyn, S.I. Bredikhin, and V.V. Kharton, *J. Solid State Electrochem.*, **16**(7), 2335 (2012).
17. S.I. Bredikhin, D.A. Agarkov, A.S. Aronin, I.N. Burmistrov, D.V. Matveev, and V.V. Kharton, *Mater. Lett.*, **216**, 193 (2018).
18. D.A. Agarkov, I.N. Burmistrov, G.M. Eliseeva, I.V. Ionov, S.V. Rabotkin, V.A. Semenov, A.A. Solovyev, I.I. Tartakovskii, and S.I. Bredikhin, *Solid State Ionics*, **344,** 115091 (2020).

19. I.N. Burmistrov, D.A. Agarkov, F.M. Tsybrov, and S.I. Bredikhin, *Russ. J. Electrochem.*, **52**(7), 669 (2016).
20. I.N. Burmistrov, D.A. Agarkov, E.V. Korovkin, D.V. Yalovenko, and S.I. Bredikhin, *Russ. J. Electrochem.*, **53**(8), 873 (2017).
21. A. Allu, A. Gaddam, S. Ganisetti, S. Balaji, R. Siegel, G. Mather, M. Fabian, M. Pascual, N. Ditaranto, W. Milius, J. Senker, D. Agarkov, V. Kharton, and J. Ferreira, *J. Phys. Chem. B.*, **22**(17), 4737 (2018).
22. A.V. Samoilov, D.A. Agarkov, and S.I. Bredikhin, *ECS Trans*., **91**(1), 1641 (2019).